

UCLA

UCLA Previously Published Works

Title

Morphology of the 12 Micron Seyfert Galaxies. I. Hubble Types, Axial Ratios, Bars, and Rings

Permalink

<https://escholarship.org/uc/item/6vq0j201>

Journal

The Astrophysical Journal, 516(2)

ISSN

0004-637X

Authors

Hunt, LK
Malkan, MA

Publication Date

1999-05-10

DOI

10.1086/307150

Peer reviewed

Morphology of the $12\ \mu\text{m}$ Seyfert Galaxies: I. Hubble Types, Axial Ratios, Bars, and Rings

L. K. Hunt

C. A. I. S. M. I. - C. N. R.

Largo E. Fermi 5, I-50125 Firenze, Italy

Electronic mail: hunt@arcetri.astro.it

and

M. A. Malkan

University of California

Department of Astronomy, 405 Hilgard Ave.,

Los Angeles, CA, 90095-1562 U.S.A.

Electronic mail: malkan@bonnie.astro.ucla.edu

ABSTRACT

We have compared the morphological characteristics of the 891 galaxies in the Extended $12\ \mu\text{m}$ Sample (E12GS), and assessed the effect of the $12\ \mu\text{m}$ selection criterion on galaxy properties. The normal spirals in the E12GS have the same axial ratios, morphological types, and bar and ring fractions as other normal spirals. The HII/starburst galaxies have a higher incidence of bars, and more than twice the normal rate of “peculiar” morphologies, both of which are attributable to relatively recent disturbances.

The $12\ \mu\text{m}$ Seyferts show a small (10%) deficiency of edge-on disks. This is caused by extinction, but is a much less severe effect than in optically-selected samples. There is a similar modest deficit of highly inclined HII/starburst galaxies in the $12\ \mu\text{m}$ sample.

The galaxies with active nuclei (AGNs: Seyferts and LINERs) have the same incidence of bars as normal spirals, but show rings significantly more often than normal galaxies or starbursts. The LINERs have elevated rates of *inner* rings, while the Seyferts have *outer* ring fractions several times those in normal galaxies. The different formation times of bars and rings suggest an interpretation of these differences. Bars form relatively quickly, and indicate that material is recently being transported (by redistribution of angular momentum) to the center of the galaxy, where it is likely to trigger a short (e.g., $\lesssim 10^8$ yrs) burst of star formation. Outer rings may result from similar disturbances, but require much more time to form. They would then be associated with more intense nuclear activity if it takes 10^9 years or more for the mass transfer to reach the center and raise the black hole accretion rate, by which time the bar has dissolved or begun to do so. Inner rings form before outer ones, with a formation time more comparable to bars. Thus it may be that after an interaction or instability triggers an infall of gas, the galaxy in the earliest stage is likely to show enhanced star formation in its center, while later it is more likely to show LINER activity, and still later likely to be a Seyfert.

The trends we find with morphology and nuclear activity are not biased either by the distances of the galaxies, or by the slightly elevated recent star formation rates shown by the $12\ \mu\text{m}$ galaxies in general.

Subject headings: Galaxies: active; Galaxies: Seyfert; Galaxies: spiral; Galaxies: starbursts; Galaxies: structure; Infrared: galaxies

1. Introduction

While for many years it was thought that initial conditions uniquely determined galaxy morphology (Eggen, Lynden-Bell, & Sandage 1962), it is now becoming apparent that morphology can be modified by physical processes (e.g., Pfenniger, Combes, & Martinet 1994). It follows that galaxy morphology can be used to study these processes, if a relationship can be established between a morphological feature and the physical mechanism responsible.

The most striking features of disk galaxy morphology are nonaxisymmetric structures such as bars and spiral patterns. Such structures can be caused by instabilities in galactic disks, and the interaction between bars and disks or bulges can give rise to angular momentum transfer and resonance phenomena. Gas, because of its dissipative properties, is expected to have a substantial influence on the development of spiral structure and bars. Numerical simulations suggest that bars can induce substantial inflows of gas (Schwarz 1981; Friedli & Benz 1993), and the consequent evolution of the bar may create thickened structures that resemble bulges (Norman, Sellwood, & Hasan 1996; Friedli & Benz 1995). Environmental effects, such as tidal interactions and mergers, can also induce bars, as well as bridges, tails, multiple nuclei, and highly non-axisymmetric “disturbed” structure. Interactions may also alter the Hubble type in spirals, causing them to evolve from late-type unbarred systems toward barred earlier types (Elmegreen, Elmegreen, & Bellin 1990).

Axisymmetric structures in galaxies, bulges and disks, may also be modified over time by these processes and others, and the Hubble sequence itself may turn out to be an evolutionary one (Pfenniger, Combes, & Martinet 1994; Martinet 1995). If this were true, there could be a link between normal spiral evolution and the triggering of starburst and nuclear (Seyfert) activity. These kinds of activity would be expected if such evolution, instead of proceeding at quiescent quasi-static rates, were to occur violently on relatively short timescales, and involve only modest fractions of the central mass.

In this paper, we investigate the morphology of several classes of disk galaxies in an attempt to better understand the physical processes behind the creation and maintenance of an active galactic nucleus (AGN). Much effort has been devoted to identifying the connection, if any, between host galaxy properties and

the AGN (Simkin, Su, & Schwarz 1980; Su & Simkin 1980; Yee 1983; MacKenty 1990; Zitelli et al. 1993; Danese et al. 1992; Granato et al. 1993; Kotilainen et al. 1992; Kotilainen & Ward 1994). In particular, galactic bars which should facilitate the inward transport of gas to fuel the active nucleus (Shlosman, Begelman, & Frank 1990) are not ubiquitous in Seyfert galaxies, even at the infrared wavelengths thought to favor bar detection (McLeod & Rieke 1995; Mulchaey & Regan 1997). Likewise, interactions are frequent in Seyferts (Dahari 1985; MacKenty 1989), but not all Seyferts are found in interacting systems (De Robertis, Yee, & Hayhoe 1998). The only salient difference between Seyfert and normal spiral *morphology* discovered to date is the near-infrared surface brightness of the disk (Hunt et al. 1998): at $2\ \mu\text{m}$, Seyfert disks turn out to be almost $1\ \text{mag arcsec}^{-2}$ brighter than those in normal early-type spirals.

This paper is the first of a series aimed at the investigation of the host-galaxy/nuclear connection in AGNs and starbursts through qualitative and then quantitative galaxy morphology. Our study is based on the Extended $12\ \mu\text{m}$ Galaxy Sample (Rush, Malkan, & Spinoglio 1993 – hereafter RMS), and here we report an analysis, with data from the literature, of the Hubble types, axial ratios, and bar and ring fractions. We also assess the impact of the infrared selection criterion on the star formation properties of the sample galaxies. Future papers will present and analyze new optical and near-infrared images of the $12\ \mu\text{m}$ Seyferts that will enable us to further quantify the morphologies of these objects.

2. The Extended $12\ \mu\text{m}$ Galaxy Sample

We have chosen the Extended $12\ \mu\text{m}$ Galaxy Sample (hereafter E12GS) for several reasons. (1) The $12\ \mu\text{m}$ selection avoids biases associated with ultraviolet selection criteria which tend to favor blue Seyfert 1s and quasars [e.g., Markarian and Green (Green, Schmidt, & Liebert 1987)]. (2) Optically-selected magnitude-limited samples may be biased against faint nuclei embedded in bright galaxies (e.g., CfA Seyfert sample: Huchra & Burg 1992), but the $12\ \mu\text{m}$ flux is an approximately constant fraction of the bolometric flux in both types of Seyferts (RMS). (3) Importantly for statistical studies, the $12\ \mu\text{m}$ Seyferts are numerous (116) and comprise the largest Seyfert sample of both types yet compiled. (4) $12\ \mu\text{m}$ Seyferts are closer than the CfA Seyferts, thus affording better

spatial resolution and higher flux densities. (5) Distances of the two types in the $12\ \mu\text{m}$ Seyferts are similar (69 Mpc for Seyfert 1s vs. 59 Mpc for Seyfert 2s) so that conclusions drawn from type comparison should not suffer from resolution or distance/luminosity effects. (6) Enhanced star formation activity may be favored by the infrared selection criterion, and evaluation of such a selection artifact may help better understand the relationship between Seyfert activity and star formation. (7) Finally, the E12GS automatically guarantees similarly-selected control samples of HII/starbursts, LINERS, and non-active galaxies.

The E12GS was defined by RMS on the basis of $12\ \mu\text{m}$ flux, and contains 891 galaxies¹. The flux limit is 0.22 Jy, and the sample is estimated to be complete to 0.3 Jy. The multiwavelength properties of Seyferts in the $12\ \mu\text{m}$ sample are discussed by Rush & Malkan (1996); Rush et al. (1996); and Rush, Malkan, & Edelson (1996). Near-infrared photometry of the galaxies in general is reported by Spinoglio et al. (1995).

3. Morphology of the $12\ \mu\text{m}$ Galaxies

We are interested in the morphological characteristics of the $12\ \mu\text{m}$ galaxies not only for their intrinsic interest, but also to assess any dependence on the $12\ \mu\text{m}$ selection criterion. Specifically, (i) what are the Hubble types of the $12\ \mu\text{m}$ galaxies, and how do they compare with those for normal spirals and previous Seyfert samples? (ii) what are the axial ratios of the $12\ \mu\text{m}$ galaxies, and how do they compare with optically-selected samples? (iii) how does the bar fraction of the $12\ \mu\text{m}$ galaxies compare with that for normal spirals, and how does it vary with activity class and Hubble type? (iv) what fraction of $12\ \mu\text{m}$ galaxies have rings?

To this end, we used the spectroscopic classifications of the E12GS (HII/starburst, LINER, Seyfert 1 or 2) from the NASA/IPAC Extragalactic Database, NED². From these classifications, three subsets of the $12\ \mu\text{m}$ galaxies were derived: HII/starburst (67 objects), LINER (33 objects), and “non-active” (neither HII/starbursts, nor LINERS, nor Seyferts: 626 objects, hereafter referred to as “normal”). Ambiguous

¹3C273 and OJ287 are not considered here.

²The NASA/IPAC Extragalactic Database (NED) is operated by the Jet Propulsion Laboratory, California Institute of Technology, under contract with the U.S. National Aeronautics and Space Administration.

designations such as HII+LINER (8 objects), HII+Sy (6), LINER+Sy (14) have been separated out in order to better represent “pure” activity classes, although we have analyzed them where necessary to evaluate the validity of possibly low-significance results.

The resulting percentage of “active” galaxies in the E12GS is roughly 30%, as opposed to the 20% value given in RMS. The increase is in large part due to the different definition and consequent greater number of HII/starbursts here, and to the inclusion of ambiguous classifications. More observations in the literature and continuous updates of NED also contribute to the increase. 29 galaxies are classified as Seyferts in NED, but are not part of the $12\ \mu\text{m}$ Seyfert samples, and, conversely, 22 of the 116 $12\ \mu\text{m}$ Seyferts are not designated as such in NED. Hence, there may be some doubt about the strict membership of the activity-class subsamples we have defined, although the samples should be large enough to submerge small random effects of mistyping.

Morphological types, bar and ring classes, and major and minor diameters were taken from NED, and the distributions of these compared among the subsets defined above. The optically-selected CfA sample of Seyferts (Huchra & Burg 1992) is also considered in the analysis, so as to better assess any selection effects introduced by the $12\ \mu\text{m}$ criterion (see § 4).

3.1. Morphological Types

The NED revised morphological types are typically taken from the Third Reference Catalogue of Bright Galaxies (RC3; de Vaucouleurs et al. 1991). The Hubble stage or type index (T) is derived from these according to the principles outlined in RC3. When an object is tagged “pec”(ulnar), but has a well-defined type, we included it in the analysis. “Peculiar” morphology is shown by only 19% of the normal $12\ \mu\text{m}$ galaxies, by roughly 25% of the $12\ \mu\text{m}$ Seyferts (21 and 27% for Types 1 and 2, respectively), by 35% of the LINERS, and by almost half (45%) of the $12\ \mu\text{m}$ HII spirals.

The distributions of Hubble type index for the different subsamples are shown in Fig. 1. It is apparent that the normal $12\ \mu\text{m}$ galaxies are predominantly spirals, as expected, and that there are fewer very late-type spirals relative to the UGC distribution (although both have median $T = 4 = \text{Sbc}$). The $12\ \mu\text{m}$ and CfA Seyfert 1s tend to be early-type spirals (median $T = 1 = \text{Sa}$), while the $12\ \mu\text{m}$ HII

galaxies and LINERs tend towards later types (medians $T = 3, 3.5 = \text{Sb, Sbc}$, respectively); Seyfert 2s are intermediate between the two with median $T = 2 = \text{Sab}$.

That Seyferts tend to reside in early-type spirals has been known for some time (Terlevich, Melnick, & Moles 1987; Moles, Márquez, & Pérez 1995). The trend found here of morphological types in Seyfert galaxies is also similar to that of the Palomar Spectroscopic Survey (Ho, Filippenko, & Sargent 1997a), and of a large sample of nearby Seyferts (Malkan, Gorjian, & Tam (1998; hereafter MGT). However, the $12\mu\text{m}$ HII galaxies tend towards earlier types and the LINERs towards later types than those detected in the Palomar survey (Ho, Filippenko, & Sargent 1997b). This may be a luminosity effect since the Palomar Survey tends towards low luminosities, or it could be related to the $12\mu\text{m}$ selection and dust or gas content. The median morphological type of both $12\mu\text{m}$ and CfA Seyfert 2s lies between Seyfert 1s and HII galaxies/LINERs (individual typing uncertainties are $T \sim 0.7$ –Buta et al. 1994), a trend confirmed by the ambiguous sub-samples: LINER/Sy galaxies have median $T = 2$, HII/Sys $T = 3$, and HII/LINERs $T = 4$. There appears to be a global progression from normal spirals and LINERS (median Sbc), to HII/starbursts (Sb), to Seyfert 2s (Sab), and Seyfert 1s (Sa).

3.2. Axial Ratios

The intrinsic shape of spiral disks may be derived from distributions of axial ratios and has been extensively studied (Sandage, Freeman, & Stokes 1970; Binney & de Vaucouleurs 1981; Fasano et al. 1993; Odewahn, Burstein, & Windhorst 1997). Here we compare the axial ratios in the E12GS with those of normal spirals, and with optically-selected Seyfert samples. The distributions of the axial ratios of the galaxies in the E12GS are shown in Fig. 2. The normal $12\mu\text{m}$ galaxies exhibit an axial-ratio distribution entirely consistent with normal disk galaxies, being roughly flat from $b/a \lesssim 1.0$ down to ~ 0.2 (Binney & de Vaucouleurs 1981).

Optically-selected Seyfert galaxies tend to avoid edge-on systems (Keel 1980), partly because of the bias of (optical) magnitude-limited samples against extremely inclined systems (Burstein, Haynes, & Faber 1991; Fasano et al. 1993; Maiolino & Rieke 1995). Indeed, the CfA Seyferts show a strong deficiency of highly inclined disks, especially for the type 1s: the

mean b/a for the CfA type 1s (2s) is 0.80 (0.77), compared with 0.56 for the normal $12\mu\text{m}$ galaxies. Figure 2 shows that the $12\mu\text{m}$ Seyfert galaxies are much less affected by this bias than the CfA sample, as the mean b/a for the $12\mu\text{m}$ type 1s (2s) is 0.65 (0.64). 11% of the type 2 Seyferts, and 13% of the type 1s have $b/a \leq 0.4$, versus none of the CfA Seyferts. A similar lack of edge-on Seyfert 2s has been noted by McLeod & Rieke (1995), who attributed it to obscuration on scales of ~ 100 pc or more.

The LINERs and HII galaxies have a mean b/a of 0.59. Only 9% of the HII galaxies have $b/a \leq 0.4$, which implies that if obscuration causes the deficiency of highly inclined galaxies, it operates equally well whether an AGN or a starburst is present.

3.3. Bars

70% of the normal sample and roughly half of each of the active samples have bar classes defined, and those galaxies with bar definitions have been divided into three categories: unbarred (SA); barred (SAB or SB); and strongly barred (SB). Table 1 gives the results of this division. It turns out that 69% of the normal galaxies are barred, in good agreement with the magnitude-limited sample of northern spirals with $B \leq 13$ of which 68% have bars (see Moles et al. 1995), but slightly higher than the 60% fraction in field spirals (Sellwood & Wilkinson 1993) and in the Palomar Survey spirals (Ho, Filippenko, & Sargent 1997c). If we apply a velocity constraint and consider only those sources with $v < 5000 \text{ km s}^{-1}$, the bar fraction is 68%. We conclude that the bar properties of the $12\mu\text{m}$ normal galaxies are similar to those of optically-selected samples (see also Pompea & Rieke 1990).

In contrast to the normal spirals, the vast majority of the $12\mu\text{m}$ starbursts are barred. 82–85% (depending on whether the distant galaxies are excluded) of the HII/starbursts with known bar class are barred, and half of them are strongly barred³. This is a significantly higher barred fraction of HII galaxies than the 61% found by Ho et al. (1997c), and it does not appear to be a selection effect. A detailed discussion of barred starbursts or star formation in barred galaxies is beyond the scope of this paper, but it would appear that all starbursts, at least relatively luminous ones, are preferentially barred. We have analyzed the bar

³The hybrid HII/Sy sample with defined bar class has 4 of 4, or 100%, barred, while the HII/LINERs have 4 of 7 barred (57%).

TABLE 1
BAR CLASS AND ACTIVITY TYPE

Activity Type	Total ^a	Unbarred (SA)	Weakly Barred (SAB)	Strongly Barred (SB)	Barred (SAB + SB)
Normal	447	138 (31%)	131 (29%)	178 (40%)	309 (69%)
HII/starburst	34	5 (15%)	11 (32%)	18 (53%)	29 (85%)
LINER	23	9 (39%)	9 (39%)	5 (22%)	14 (61%)
12 μ m Sy 1	28	9 (32%)	12 (43%)	7 (25%)	19 (68%)
12 μ m Sy 2	33	11 (33%)	9 (27%)	13 (39%)	22 (67%)
CfA Sy 1	18	8 (44%)	5 (28%)	5 (28%)	10 (56%)
CfA Sy 2	12	4 (33%)	5 (42%)	3 (25%)	8 (67%)
<i>v</i> < 5000 km s ⁻¹ ⇒					
Normal	401	128 (32%)	122 (30%)	151 (38%)	273 (68%)
HII/starburst	28	5 (18%)	10 (36%)	13 (46%)	23 (82%)
LINER	23	9 (39%)	9 (39%)	5 (22%)	14 (61%)
12 μ m Sy 1	20	6 (30%)	9 (45%)	5 (25%)	14 (70%)
12 μ m Sy 2	27	10 (37%)	6 (22%)	11 (41%)	17 (63%)
CfA Sy 1	11	4 (36%)	5 (45%)	2 (18%)	7 (64%)
CfA Sy 2	6	2 (33%)	2 (33%)	2 (33%)	4 (67%)

^aTotal number of objects with well-defined bar class.

fraction of the Markarian nuclear starbursts (as listed by Balzano 1983 and by Mazzarella & Balzano 1986) and found that 87.5% of the (32) galaxies with known bar class are barred, and 75% are strongly barred.

The bar fractions of $12\mu\text{m}$ LINERs and Seyferts appear very normal with between 61 and 68% of them having bars; the CfA Seyferts are similar with roughly a 62% bar fraction. 4 of 9 hybrid LINER/Sy are barred (56%). This is yet another confirmation of the emerging consensus that bars occur in Seyferts with the same frequency as they occur in the normal spiral population (see Introduction and references therein). Recent work has suggested that bars and distortions are more frequent in type 2 Seyferts than in type 1s (Maiolino et al. 1997). For the $12\mu\text{m}$ Seyferts, however, this is not the case as the bar fraction (with $v < 5000\text{ km s}^{-1}$) is greater for type 1s (70%) than for type 2s (63%). It is only marginally the case for the CfA sample which has 67% of Seyfert 2s barred versus 64% of Seyfert 1s, although if all distances are considered, the differences between the two types in the CfA sample are more pronounced (56% type 1s vs. 67% type 2s, see Table 1). More and higher-quality image data are needed to decide if the difference is significant, and if so, if it results from optical selection.

We turn finally to the variation of bar fraction with morphological type. Although the counting statistics are sufficiently large only for the normal sample, we have analyzed bar fraction as a function of Hubble type as shown in Fig. 3; the data have been binned as described in the figure caption. Very late-type normal E12GS galaxies show a higher percentage of bars than early types, as also found by Ho et al. (1997c): 86% (31/36) of the $12\mu\text{m}$ galaxies with $T > 6$ are *strongly* barred (SB), and only 8% (3/36) are not barred at all. Otherwise the bar fraction is constant with morphological type, except for S0s and earlier, which tend to have a lower percentage (see also Ho et al.).

Within the errors, the bar fractions of $12\mu\text{m}$ HII galaxies and Seyfert 2s are also constant with morphological type, while Seyfert 1s show a peak of 90% at type Sb ($T = 3$). This type is also the mode in the Hubble type distribution, and means that 9 of 10 Sb Seyfert 1s are barred. The fraction of unbarred Seyfert 1s is highest for the very early-types (S0 and earlier), similar to the case for normal galaxies.

3.4. Rings

Rings trace dynamical resonances in galaxies and are locations of strong density enhancements in stars and gas. Numerical simulations show that bar perturbations can form rings (Schwarz 1981), and almost inevitably do in early-type spirals (Combes & Elmegreen 1993; Piner et al. 1995). Patterns in ring structure have also been interpreted as an evolutionary sequence in Seyferts where rings signify active gas flow into nuclear regions (Su & Simkin 1980). For these reasons, we have quantified the presence of rings in the E12GS. Inner and outer rings have been associated with inner and outer Lindblad resonances (Schwarz 1981; Buta 1993; Piner et al. 1995), and we have used the RC3 designations “(*r*)” and “(*rs*)” to tally inner rings, and “(*R*)” and “(*R'*)” for outer ones. The tallies are shown in Table 2, together with the (*s*) (S shape), which designates an inner spiral. Following Simkin et al. (1980), we have applied a velocity constraint ($v < 5000\text{ km s}^{-1}$), shown in the lower part of the Table and in Fig. 4, so as to ensure reasonably consistent typing among the different activity types.

Outer rings are relatively rare in normal galaxies, as shown in Table 2. Simkin et al. (1980) found similar fractions for an optically-selected comparison sample of normal spirals, so the $12\mu\text{m}$ galaxies appear normal in terms of the occurrence of rings. Three features, however, stand out in Table 2: (1) the high fraction of Seyferts – especially type 1s – with outer rings (40% for $v < 5000\text{ km s}^{-1}$, as opposed to 10% for the normal $12\mu\text{m}$ galaxies); (2) the high fraction of Seyferts and LINERs with both inner and outer rings; and (3) the high fraction of LINERs with inner rings. Seyferts show outer rings or simultaneous inner and outer ring structures between 3 and 4 times more frequently than do normal spirals; the formal significance of the higher Seyfert 1 outer ring fraction is 3.9σ . Outer rings occur in LINERs almost twice as often as normal, although with low significance, and with a normal frequency in HII/starburst galaxies. No outer rings are found in any of the hybrid activity classes, although S shapes occur in 70% of the HII hybrids (HII/LINER, HII/Sy). The anomalously high outer ring fraction in Seyferts is similar to results reported for Simkin et al. (1980) for a smaller optically-selected sample. The incidence of inner rings (40%) and S shapes (33%) in normal spirals (see also Simkin et al. 1980) is exceeded only by the LINERs (57%), a $2\text{-}\sigma$ effect. MGT also found that inner rings are not unusually frequent in Seyfert galaxies.

TABLE 2
RING CLASS AND ACTIVITY TYPE

Activity Type	Total ^a	Outer Ring (R) + (R')	Inner Ring (r) + (rs)	Outer + Inner ^b	Outer Inner ^c	S-shaped (s)
Normal	547	58 (11%)	209 (38%)	36 (7%)	237 (43%)	174 (32%)
HII/starburst	47	2 (4%)	18 (38%)	2 (4%)	18 (38%)	13 (28%)
LINER	29	4 (14%)	13 (45%)	3 (10%)	14 (48%)	8 (28%)
12 μ m Sy 1	34	10 (29%)	13 (38%)	6 (18%)	17 (50%)	12 (35%)
12 μ m Sy 2	45	11 (24%)	14 (31%)	5 (11%)	21 (47%)	11 (24%)
CfA Sy 1	19	6 (32%)	6 (32%)	2 (11%)	10 (53%)	10 (53%)
CfA Sy 2	16	3 (19%)	7 (44%)	3 (19%)	7 (44%)	1 (6%)
$v < 5000 \text{ km s}^{-1} \Rightarrow$						
Normal	479	48 (10%)	192 (40%)	31 (6%)	215 (45%)	162 (34%)
HII/starburst	36	2 (6%)	16 (44%)	2 (6%)	16 (44%)	11 (31%)
LINER	23	4 (17%)	13 (57%)	3 (13%)	14 (61%)	8 (35%)
12 μ m Sy 1	22	9 (41%)	10 (45%)	6 (27%)	13 (59%)	9 (41%)
12 μ m Sy 2	35	10 (29%)	12 (34%)	5 (14%)	18 (51%)	9 (26%)
CfA Sy 1	10	4 (40%)	4 (40%)	2 (20%)	6 (60%)	7 (70%)
CfA Sy 2	8	2 (25%)	3 (38%)	2 (25%)	3 (38%)	1 (12%)

^aNumber of objects with well-defined morphological type.

^bNumber of objects with both an inner and an outer ring.

^cNumber of objects with either an inner or an outer ring.

Because inner and outer rings may occur preferentially in very early-type barred spirals (Combes & Elmegreen 1993; Elmegreen et al. 1992), we have checked to ensure that the high outer ring fraction in Seyferts is not due to their predominantly early Hubble types. Considering only $12\ \mu\text{m}$ normal galaxies with $T \leq 2$ (Sab), the outer ring fraction increases by a factor of two (to 24%), while the inner ring fraction remains roughly constant (at 43%). Among only early types, the Seyfert outer ring fractions are 60% and 50%, for Types 1 and 2, respectively. These fractions remain significantly higher than normal, although instead of a $4\text{-}\sigma$ effect, it is around $2\ \sigma$.

We can also examine what percentage of barred and unbarred galaxies have rings, as shown in Table 3. While 10% of all normal $12\ \mu\text{m}$ galaxies have outer rings, 13% of barred normal spirals do, and 7% of the unbarred spirals. While the presence of a bar may influence the occurrence of an outer ring, bars definitely appear to be associated with inner rings: 52% of barred spirals have inner rings, but only 38% of unbarred spirals have them. Such a result is not surprising since inner resonances are expected to develop in early-type barred spirals (Combes & Elmegreen 1993). These fractions for $12\ \mu\text{m}$ spirals are consistent with those reported by de Vaucouleurs & Buta (1980) who find a fraction of 43% of the unbarred and almost 70% of the barred spirals in the Second Reference Catalogue of Bright Galaxies (RC2; de Vaucouleurs, de Vaucouleurs, & Corwin 1976) to have inner rings. Finally, twice the normal fraction ($\gtrsim 80\%$) of *unbarred* HII/starburst galaxies have inner rings.

3.5. Morphology Summary

We have examined the attributes, gleaned from NED, of the E12GS, and find:

- i.* The normal spirals in the E12GS are truly normal in terms of morphological types, axial ratio distribution, bar fraction, and rings. Only one-fifth (19%) of them are designated as morphologically “peculiar”.
- ii.* Almost half (45%) of the $12\ \mu\text{m}$ HII/starburst galaxies are morphologically “peculiar”, and more than 80% of them are barred. A normal percentage of them has rings, but twice the normal fraction ($\gtrsim 80\%$) of unbarred HII/starbursts show inner rings.

- iii.* The axial ratios of the $12\ \mu\text{m}$ Seyferts show a much smaller deficiency of edge-on systems than in optically-selected Seyferts. This is because selection in the mid-infrared is much less biased against Seyferts suffering large extinction.

- iv.* One-fourth of the $12\ \mu\text{m}$ Seyferts are classified as having “peculiar” morphology, and, consistently with previous studies, they are not preferentially barred.

- v.* The incidence of outer rings and simultaneous inner/outer rings in the $12\ \mu\text{m}$ Seyferts is overwhelmingly higher ($\times 3\text{--}4$) than that for normal spirals; LINERs show a high ($\times 1.5$ normal) inner ring fraction. Both results are statistically significant.

4. Star Formation in the $12\ \mu\text{m}$ Sample

An important selection effect that may operate in the E12GS is the tendency for infrared-selected galaxies to be dominated by powerful star formation (e.g., Soifer et al. 1987). Star formation occurring on short timescales can alter morphology, and thereby flavor results drawn from a morphological analysis. Such a selection artifact could also influence conclusions about star formation and Seyfert activity. For these reasons, we have attempted to quantify star formation in the E12GS on the basis of infrared luminosity ratios and colors.

4.1. Infrared-to-Blue Luminosity Ratio

Infrared (IR) emission measured by the *Infrared Astronomical Satellite* (IRAS) is usually attributed to dust heated by the quiescent interstellar medium (20–25 K), young massive stars (~ 50 K), and possibly an AGN (e.g., Rowan-Robinson & Crawford 1989). The relative contribution of these processes determines the infrared luminosity output which can vary substantially from galaxy to galaxy. As the contrasting examples of M 31 and Arp 220 illustrate (Telesco 1988), infrared-to-blue luminosity ratios (L_{IR}/L_B) range over a factor of 1000 (e.g., Soifer et al. 1984). Although L_{IR}/L_B is not a direct measure of “infrared activity” in galaxies (Soifer et al. 1989), it is commonly used as an indicator of the relative importance of young stars and vigorous star formation (Keel 1993; Combes et al. 1994), and we have calculated L_{IR}/L_B for the sample galaxies. For the far-infrared (FIR) contribution (from 40 to $120\ \mu\text{m}$), we used the

TABLE 3
BARS WITH RINGS AND ACTIVITY CLASS^a

Activity Type	$(R) + (R')$		$(r) + (rs)$	
	Barred ^b	Unbarred ^b	Barred ^b	Unbarred ^b
Normal	36 (13%)	9 (7%)	142 (52%)	49 (38%)
HII/starburst	1 (4%)	1 (20%)	12 (52%)	4 (80%)
LINER	2 (14%)	2 (22%)	8 (57%)	5 (56%)
12 μ m Sy 1	8 (57%)	1 (17%)	9 (64%)	1 (17%)
12 μ m Sy 2	8 (47%)	2 (20%)	10 (59%)	2 (20%)
CfA Sy 1	4 (57%)	0 (0%)	4 (57%)	0 (0%)
CfA Sy 2	1 (25%)	1 (50%)	2 (50%)	1 (50%)

^aWith $v < 5000 \text{ km s}^{-1}$.

^bPercentages are calculated using total number with a given bar class. (See Cols. (3) and (6) of Table 1.)

usual expression: $FIR = 3.25 \times 10^{-14} f_{\nu}(60 \mu\text{m}) + 1.26 \times 10^{-14} f_{\nu}(100 \mu\text{m})$ (e.g., Persson & Helou 1987). The B -band contribution was calculated as νf_{ν} based on the magnitudes given in NED, taken mostly from RC3.

Figure 5 shows the distributions of L_{IR}/L_B for the various activity classes of the E12GS. The normal galaxies in the E12GS are characterized by L_{IR}/L_B (median log of 0.16) intermediate between the high ratios typical of infrared-selected galaxies selected at 60 μm (IRAS Bright Galaxy Sample –BGS– Soifer et al. 1987; the median (log) of 0.75 is shown by the right vertical arrow in the lowest panel of Fig. 5), and the low ratios in optically-selected galaxies [de Jong et al. 1984, medians (log) of -0.4 (unbarred) and -0.26 (barred) shown by the left arrows]. We conclude that the tendency of infrared selection criteria to favor high L_{IR}/L_B is much less pronounced at 12 μm than at 60 μm .

The 12 μm -selected Seyferts have higher L_{IR}/L_B (median log: -0.05, 0.31 for type 1s and 2s, respectively) than their optically-selected CfA counterparts (-0.14, 0.13 for the CfA Sy 1s, 2s); Seyfert 2s in both samples show higher values of L_{IR}/L_B than in Seyfert 1s. The 12 μm HII/starbursts have a median (log) L_{IR}/L_B (0.55) larger than any of the other classes, comparable only to the BGS, while 12 μm LINERS show the lowest L_{IR}/L_B of any of the 12 μm activity

classes, similar to those in Seyfert 1s. Although these results seem to indicate a moderate 12 μm selection effect on Seyferts, some fraction of the Seyfert 60 μm flux can be due to the AGN (Spinoglio et al. 1995). Such a contribution would boost L_{IR}/L_B , independently of recent star formation history.

4.2. The Proportion of Warm and Cold Dust Components

IRAS observations revealed that infrared-to-blue luminosity ratios correlate with the flux ratio $\Theta \equiv f_{\nu}(60\mu)/f_{\nu}(100\mu)$ (de Jong et al. 1984), although the correlation is looser in IR-selected samples (Soifer et al. 1984). This was probably the first observational evidence of the presence of a cold dust component and a more variable warm component: the higher the 60 $\mu\text{m}/100 \mu\text{m}$ ratio, the higher the proportion of warm dust, and the more L_{IR} emitted relative to the optical. Such correlations are shown for the E12GS in Fig. 6. The two bold data points in the Normal panel show the loci of optically-selected samples (lower left, de Jong et al. 1984), and 60 μm -selected ones (upper right, Soifer et al. 1989). It can be seen that the normal 12 μm galaxies are well-represented by these values, while almost half of the HII/starbursts exceed them. On the other hand, more Seyferts fall below the normal range than above it, and they show the worst correlation of any of the activity classes.

Subsequent work demonstrated that IR emission from the interstellar medium (ISM), the cold component, is not well-represented by “classical” dust grains in thermal equilibrium (silicate and graphite particles with diameters ranging from 0.005 to 0.25 μm), as they fail to produce the observed emission for $\lambda < 40 \mu\text{m}$ (Pajot et al. 1986). Very small grains transiently heated by the absorption of single UV photons were proposed by Sellgren (1984) to explain the excess mid-infrared emission. In galaxies, a general relationship between IRAS color ratios $f_\nu(60\mu)/f_\nu(100\mu)$ and $f_\nu(12\mu)/f_\nu(25\mu)$ was found by Helou (1986), and interpreted as the interplay between the contributions from classical and very small grains. Indeed, an empirical estimate of the small-to-large dust grain ratio $\Gamma \equiv \nu f_\nu(12\mu)/FIR$ has been shown to depend only on the flux ratio Θ in Galactic nebulae and in optically- and IR-selected samples of galaxies (Helou, Rytter, & Soifer 1991; hereafter HRS).

Given that the E12GS is defined on the basis of 12 μm flux, the selected galaxies may be anomalous in their dust content or relative contributions from the large and small dust grains. We have therefore considered the behavior of Γ , the ratio of 12 μm flux to FIR, in the sample galaxies. Following HRS, Fig. 7 shows Γ versus Θ for the various activity classes in the E12GS. The phenomenological model described in HRS, and plotted in Fig. 7, consists of two dust phases: a cool one represented with a quiescent ISM energy density of $u_c \simeq 0.5 \text{ eV cm}^{-3}$, and the other with an increasing fraction immersed in a higher intensity field $u_w \simeq 30 \text{ eV cm}^{-3}$ (solid line), or $u_w \simeq 100 \text{ eV cm}^{-3}$ (dotted line). Also shown in Fig. 7 as a dashed line in the lower left panel is the linear fit to data from the Galactic interstellar medium in the vicinity of stars as given by HRS. The remaining panels in Fig. 7 show as a dot-dashed line the colors that would be observed were the quantities artificially controlled by the 12 μm flux limit; such a trend is not followed by the data. The figure shows convincingly that the HRS two-phase dust model is appropriate for the bulk of the normal galaxies, the LINERS, and the HII/starbursts, except, perhaps at high Θ .

To assess the influence of star-formation properties on the morphological characteristics described in the previous section, we have calculated the fractions of bars and rings in “star-forming” and “quiescent” galaxies in the E12GS, as distinguished by the far-infrared flux ratio Θ . The median value of the HII/starbursts was used as the threshold: $\Theta = 0.51$;

galaxies with the far-infrared flux ratio greater than this value were (arbitrarily) considered “star-forming”, and the others “quiescent”. With this criterion, 20% of the normal 12 μm galaxies turn out to be actively star-forming, and 50% of the HII/starbursts (by definition), 13% of the LINERS, 30% of the Seyfert 1s, and 56% of the Seyfert 2s. The occurrence of bars in the star-forming galaxies is significantly (4.8σ) higher than the quiescent category (86% versus 63%) only for the normal galaxies; there is no equivalent trend for HII/starbursts, LINERS, or Seyferts.

Normal star-forming galaxies also have a higher percentage of *outer* rings than their quiescent counterparts (24% versus 8%), with a significance of 2.4σ ; the same is true for Seyfert 1s (83% versus 28%, 3σ), but not for Seyfert 2s (40% versus 33%). An opposing trend emerges for *inner* rings, with quiescent normal galaxies having a higher inner ring fraction (50%) than the star-forming ones (37%), an effect which is only marginally significant at 2.1σ . The same is true for Seyfert 2s (66% quiescent versus 27% star-forming, significance 2.2σ), but not for Seyfert 1s. Evidently outer rings tend to prefer “actively-star-forming” galaxies, while inner ones prefer quiescent ones⁴. Nevertheless, even the quiescent Seyferts have outer ring fractions of around 30%. We conclude then that the high outer ring fraction found in Seyferts is not an artifact of the the 12 μm selection criterion, which may favor more recent star formation.

4.3. Mid-Infrared Flux Ratio

The HRS model for dust emission does *not* apply to the majority of Seyfert galaxies, mostly because of the excess at 25 μm that characterizes the objects in the upper right corner of the Seyfert panel in Fig. 7⁵. Indeed, the mid-infrared flux ratio $f_\nu(25\mu)/f_\nu(60\mu)$ in the 12 μm Seyferts correlates extremely well with Γ , but not with L_{FIR}/L_B or with L_{FIR} , unlike optically-selected Seyferts where smaller $f_\nu(25\mu)/f_\nu(60\mu)$ is associated with higher L_{FIR} (Hunt 1991). The large deviation from the dust model in Fig. 7 must therefore arise from the mid-infrared excess observed in Seyferts (Miley, Neugebauer, & Soifer 1985; Edelson & Malkan 1986), attributed to an AGN, either emis-

⁴87% of the LINER sample is quiescent, and also has the highest inner ring fraction of any of the activity classes.

⁵Large values of the $f_\nu(25\mu)/f_\nu(60\mu)$ flux ratio were used initially to define potential Seyfert samples (de Grijp, Miley, & Lub 1987).

sion directly from the nucleus or from dust heated by it.

We have also examined the “warm” and “cold” fractions of the $12\ \mu\text{m}$ galaxies on the basis of the mid-infrared flux ratio $f_\nu(25\mu)/f_\nu(60\mu)$. Following Soifer et al. (1989), we distinguish between “warm” and “cold” with $f_\nu(25\mu)/f_\nu(60\mu) = 0.17$, and find 21% of the normal $12\ \mu\text{m}$ galaxies to be warm, as opposed to the 16% fraction in the $60\text{-}\mu\text{m}$ selected BGS. This higher percentage is almost certainly due to the $12\ \mu\text{m}$ flux selection criterion because of the correlation between $f_\nu(12\mu)$ and $f_\nu(25\mu)$. The warm fractions of HII/starbursts (18%) and LINERs (13%) are similar to the BGS, while the much greater fractions (almost 60%) of warm Seyferts arise from the mid-infrared excess cited above.

We have investigated the occurrence of rings and bars in warm and cold galaxies in the E12GS. It turns out that the ring fractions in HII/starbursts and LINERs are similar for warm and cold objects, but the outer ring fraction in warm normal $12\ \mu\text{m}$ galaxies is greater (17%) than in cold ones (9%), a significant trend at $3.1\text{-}\sigma$. A similar conclusion holds for the outer rings in Seyferts: 54% (50%) of warm Seyfert 1s (2s) have outer rings, versus 33% (18%) of cold Seyferts, but only the difference in Seyfert 2s is marginally significant at 1.9σ . It therefore seems plausible to interpret the higher outer ring fractions in warm normal $12\ \mu\text{m}$ galaxies as due to unidentified Seyferts, seen also in the Normal panel in Fig. 7 as the vertically-displaced outliers. There are no significant differences in the bar frequencies between warm and cold $12\ \mu\text{m}$ galaxies of any activity class. We conclude then that even though 1/5 of the E12GS is “warm”, as opposed to 1/6 of the $60\text{-}\mu\text{m}$ selected BGS, the ring and bar fractions do not depend significantly on mid-infrared flux ratio, except perhaps as it relates to Seyfert activity.

4.4. Star Formation Summary

The analysis of the infrared properties of the E12GS reveals that:

- i.* The L_{FIR}/L_B ratios of galaxies in the E12GS are intermediate between optically-selected and $60\ \mu\text{m}$ -selected samples, but tend to be higher in the HII/starbursts and in the Seyfert 2s.
- ii.* While the high values of L_{FIR}/L_B and the general properties of the infrared emission in $12\ \mu\text{m}$

normal galaxies, LINERs, and HII/starbursts can be explained by the two-phase dust model proposed in HRS, those of Seyferts cannot.

- iii.* Deviations from the dust model in Seyferts seems to be due to their excess emission at $25\ \mu\text{m}$, thought to have origin in either dust heated by the AGN, or in the AGN itself.
- iv.* Bar fractions in the E12GS are significantly greater for greater far-infrared flux ratio $f_\nu(60\mu)/f_\nu(100\mu)$ *only for the normal galaxies*; no class shows a dependence of bar fractions on $f_\nu(25\mu)/f_\nu(60\mu)$.
- v.* Outer rings in normal galaxies and Seyferts tend to prefer higher $f_\nu(60\mu)/f_\nu(100\mu)$ and $f_\nu(25\mu)/f_\nu(60\mu)$ ⁶, while for inner rings the reverse is true. Nevertheless, the high outer ring fractions in Seyferts and the high inner ring fraction in LINERs do not appear to be the result of a selection artifact.

These considerations lead us to conclude that the $12\ \mu\text{m}$ selection criterion does influence the star-formation activity of the E12GS, but the effect is mild compared to that of $60\ \mu\text{m}$ selection. Not unexpectedly, the $12\ \mu\text{m}$ HII/starbursts display extreme values of the “star-formation” indicators, but they are compatible with trends predicted by two-component dust models. The infrared properties of the $12\ \mu\text{m}$ Seyferts may be partly affected by recent star formation activity, at least in Seyfert 2s, but there is undeniably a strong contribution from an AGN, since Γ correlates very well with the mid-infrared flux ratio $f_\nu(25\mu)/f_\nu(60\mu)$, known to be an indicator of Seyfert activity.

5. Interpretation and Implications

We have examined the morphological attributes and global star-formation characteristics of the 891 galaxies in the E12GS. In what follows, we attempt to link together some of the results, and provide a coherent picture of what they might imply for galaxies hosting AGNs and starbursts in particular, and for spiral galaxies in general.

5.1. How Many AGN Do We Miss from Extinction in the Galactic Disk?

If we simply assume that the *intrinsic* distribution of b/a in the Seyfert host galaxies must be uniform,

⁶The former significantly for Seyfert 1s, while the latter for Seyfert 2s.

like what we observe in the normal $12\ \mu\text{m}$ galaxies, we can estimate how many inclined Seyferts are missing from the $12\ \mu\text{m}$ sample. Even if *all of the Seyferts* within the flux limit were picked up by the E12GS, the identification of their Seyfert nuclei still rests on optical spectroscopy, which could be incomplete in the presence of large extinction in the body of the host galaxy. The b/a distributions of the $12\ \mu\text{m}$ Seyfert 1s and 2s can be made identical to that of the normal galaxies with the addition of 5 highly inclined ($b/a < 0.4$) Seyfert 1s, and 5 highly inclined Seyfert 2s. This corresponds to incompletenesses of 12% and 9% for the Seyfert 1s and 2s, respectively. This may be however an overestimate, especially for type 1s with a median Hubble type of Sa, since the axial-ratio distributions of the $12\ \mu\text{m}$ Seyferts are very similar to those of normal early-type spirals (Binney & de Vaucouleurs 1981).

5.2. Why are Outer Rings but not Bars Abnormally Frequent in Seyfert Nuclei?

Previous researchers suggested that, since many reasonably-sized galaxies already harbor massive black holes, perhaps from their early formation days, the key to making them Seyferts is a gas supply that can fuel their nucleus during the current epoch. Alternatively, black holes could be formed and maintained by normal stellar evolution in a massive compact nuclear star cluster (Norman & Scoville 1988). Either way, any dynamical mechanism that can redistribute angular momentum, and cause gas to spiral in very close to the center, should be strongly associated with central bursts of star formation and observed nuclear activity.

Bars, or nested bars, are thought to be such a mechanism. In fact they probably *do* function in this way, because they seem to be helpful in promoting a burst of star formation in the center of a “normal” galaxy, as indicated in §3. However, it is not understood why bars do *not* promote Seyfert nuclear activity, even in any weak statistical sense.

One answer to this dilemma may lie in the large fraction of outer rings in Seyferts. Buta & Combes (1996) discuss the observational and theoretical properties of rings in spiral galaxies, and we mention here a few points germane to our discussion but not already mentioned previously. First, bars in galaxies require between 2 and 5×10^8 yrs to form (Combes & Elmegreen 1993); subsequently, formation of nuclear and inner rings requires roughly 10^8 yrs, and outer

rings about 3×10^9 yrs. Second, while outer rings (R) can be sustained for a Hubble time in the absence of tidal interactions, in dense environments they are relatively fragile and tend to be either completely destroyed or converted into pseudo-rings (R'). Third, inner or nuclear rings can have a lifetime as short as 10^8 yrs, because of nuclear gas inflow and consequent star formation. Fourth, because of the long time necessary for the formation of an outer ring, true outer rings⁷ would not be expected to be observed preferentially in strongly barred galaxies. This last is true because strong bars are thought to be only a transient phase in the life of the galaxy, as they can be dissolved or converted into lenses or triaxial configurations by massive gas flow to the center. It follows that rings may supplant bars as signals of historical angular momentum transfer late in the life of the galaxy. Seyfert galaxies, with their high ring frequency, may have reached an advanced stage in their evolution which would be characterized by “older” indicators of angular-momentum transfer.

Such timescale considerations would also help explain the extremely high bar fraction in HII/starburst galaxies. If bars, associated with centralized starbursts, signal mass transfer *only early on in the galaxies’ development*, then we could interpret the low outer-ring fraction in HII galaxies as an indication of lack of time; outer rings have not yet had time to form in starbursts. On the other hand, 80% (of the 20%) *unbarred* HII fraction present inner rings; such structures would have had sufficient formation time if the timescales delineating “early” and “late” (or young and old) are roughly 10^8 and 10^9 yrs, respectively. An implication of this scenario is that the “trigger delay time” for Seyfert activity should be much longer than that for starbursts.

5.3. Implications for AGN Unification

The core idea of AGN Unification schemes is that apparently different types of nuclear activity may in fact be intrinsically similar, if only we could observe them more fully. Two examples of AGN unification are the hypotheses that: *i*) the emission lines in “classical” LINERs are photoionized by a hard continuum, the same as in Seyfert 2 nuclei, except that the ionization parameter is lower because of the lower intensity of radiation reaching the emitting clouds; or *ii*) each narrow-line AGN (e.g. Seyfert 2) actually contains a

⁷As opposed to pseudo-outer rings which appear to be younger.

broad-line region like those in Seyfert 1s, but something obscures it from our view.

One implication of the unification hypotheses is that the apparently different types of active nuclei should reside in statistically similar galactic environments. In other words, the host galaxy should not “make much difference” to the AGN, if they are all fundamentally the same kind of objects. Thus a (negative) test is proposed: are there any significant differences between the host galaxies of different classes of AGNs? As usual, the most difficult aspect of such tests is finding suitably unbiased samples, so that apparent differences are not artificially produced by selection effects.

This was a strong motivation for our morphological study of the host galaxies of the $12\mu\text{m}$ AGN. In terms of bars, the $12\mu\text{m}$ AGN pass the unification test, since we could not find any significant differences among AGN types. In contrast, the HII-region galaxies show a higher bar frequency. In this regard, then, LINER galaxies resemble more the Seyferts than the HII/starbursts.

In our relatively unbiased AGN sample, we found apparent host-galaxy differences among different AGN types: *i*) The LINERs appear to have an unusually high incidence of *inner* ($\sim 10^8$ yrs formation time) rings, in contrast to the Seyfert 1s which have an unusually high incidence of *outer* ($\sim 10^9$ yrs formation time) rings. This complicates the simplest version of unification for LINERs and Seyferts. One possible embellishing solution, for example, might be to postulate that LINER and Seyfert nuclei are the same objects, but seen at different evolutionary stages, as revealed by the differences in the rings in their host galaxies (see above). *ii*) The Seyfert 2s appear to have later morphological types than Seyfert 1s. Again a possible complication could be that Seyfert 2 nuclei are dustier, creating more obscuration along more lines-of-sight (see discussion in MGT).

We could carry the proposed negative test further by formulating a counter-hypothesis: Seyfert, LINER, and starburst activity in galaxies could be directly related to the evolutionary status of the galaxy, at least since its last major disturbance. Previous work (see Introduction) suggests that non-axisymmetric perturbations, such as bars, induce rapid evolution of spiral disks through transfer of angular momentum; evolution in this sense is most likely from late to early spiral types (Pfenninger 1993; Martinet 1995). The presence of gas is fundamental in this process

because of its dissipative properties and destabilizing influence.

It follows that Seyfert nuclei, hosted by predominantly early-type spirals, would represent a more evolved manifestation of activity (central gas deposit) than either LINERs or starbursts which tend to be found in later Hubble types. Type 1 Seyferts would also be older, more evolved, than type 2s since they are found in slightly earlier morphological types. The high frequency of outer rings in Seyferts, inner rings in LINERs, and bars in HII/starbursts would also follow, since the different formation times and lifetimes of these structures would reflect differences in the evolutionary stage of the galaxies. If peculiar morphologies reflect recent (young) disturbances, likely since they occurred more frequently in the past (van den Bergh 1998, and references therein), then the peculiar fractions that decrease systematically going from HII/starbursts (45%), to LINERs (37%), Seyfert 2s (27%), and Seyfert 1s (21%) obey a similar trend in evolutionary status. The high HI mass fractions in starbursts that decrease going to Seyfert 2s and 1s, together with an opposing trend in disk surface brightness (Hunt et al. 1998) are also compatible with such a progression of activity and Hubble type. Finally, an evolutionary sequence from starbursts to Seyfert 2s, to type 1s (e.g., Oliva et al. 1995) would be a possible consequence.

In the same vein, if Seyfert 2 nuclei were younger/less evolved than type 1s, and considering that type 2 nuclei tend to be weaker relative to the galaxy than type 1s (Yee 1983), we would deduce that the intensity of nuclear activity increases with age. If age goes hand-in-hand with morphological type, we might therefore expect to find trends with measures of nuclear activity. Figure 8, where the mid-infrared flux ratio $f_\nu(25\mu)/f_\nu(60\mu)$ is plotted against the Hubble type index, may show such a trend. As discussed in § 4.3, $f_\nu(25\mu)/f_\nu(60\mu)$ is a good indicator of Seyfert activity, and the figure shows a correlation between it and Hubble type T; the correlation is significant at $> 99.9\%$ (two-tailed). As the mid-infrared flux ratio becomes larger, the morphological types become earlier, and the nuclei older and more intense, if time increases to the left as it would were our hypothesis correct. If $f_\nu(25\mu)/f_\nu(60\mu)$ measures black hole mass, presumably related to nuclear intensity, such a trend would also be consistent with the correlation between black hole mass and total bulge luminosity (Kormendy & Richstone 1995), since early-type

spirals tend to have more luminous bulges than late types.

While our findings are inconsistent with some of the consequences of the Unification Scheme for AGNs, and perhaps more consistent with other hypotheses, our study suffers from limitations. We have used qualitative data from the literature, and some of the results are of necessity plagued by small-number statistics. High-quality multiwaveband image data are needed to systematically quantify the occurrence of bars, rings, and lenses, and to better evaluate their influence on the galaxy as a whole. Indeed, lenses may follow from bar dissolution (Combes 1996), but the lack of consistent literature data in this regard precluded analysis. A subsequent paper will report on an optical and near-infrared image atlas of the $12\ \mu\text{m}$ Seyferts with the aim of further investigating the connection between nuclear activity and galaxy morphology.

This research was partially funded by ASI Grant ARS-98-116/22. One of us (M.A.M.) would like to thank the Italian National Astronomy Group (G.N.A. – C.N.R.) and the Osservatorio Astrofisico di Arcetri for financial support. Extensive use was made of the NASA/IPAC Extragalactic Database (NED), operated by the Jet Propulsion Lab, Caltech, under contract with NASA. We thank Brian Rush for providing tabulations of some of the IRAS data, and Roberto Maiolino for stimulating discussions. Finally, we are grateful to the referee Susan Simkin for helpful suggestions and insightful comments.

REFERENCES

- Balzano, V.A. 1983, ApJ, 268, 602
- Binney, J., & de Vaucouleurs, G. 1981, MNRAS, 194, 679
- Burstein, D., Haynes, M.P., & Faber, S.M. 1991, Nature, 353, 515
- Buta, R. 1993, PASP, 105, 654
- Buta, R., Mitra, S., de Vaucouleurs, G., & Corwin, H.G., Jr. 1994, AJ, 107, 118
- Buta, R., & Combes, F. 1996, *Fundamentals of Cosmic Physics*, 17, 95
- Combes, F., & Elmegreen, B.G. 1993, A&A, 271, 391
- Combes, F., Prugniel, P., Rampazzo, R., & Sulentic, J.W. 1994, A&A, 281, 725
- Combes, F. 1996, in *Barred Galaxies*, Buta, R., Crocker, D.A., & Elmegreen, B.G. eds., ASP Conference Ser. Vol. 91, 286
- Dahari, O. 1985, AJ, 90, 1772
- Danese, L., Zitelli, V., Granato, G.L., Wade, R., De Zotti, G., & Mandolesi, N. 1992, ApJ, 399, 38
- de Grijp, M.H.K., Miley, G.K., & Lub, J. 1987, A&AS, 70, 95
- De Jong, T., Clegg, P.E., Soifer, B.T., Rowan-Robinson, M., Habing, H.J., Houck, J.R., Aumann, H.H., & Raimond, E. 1984, ApJ, 278, L67
- De Robertis, Yee, H.K.C., & M.M., Hayhoe, K. 1998, ApJ, 496, 93
- de Vaucouleurs, G., de Vaucouleurs, A., & Corwin, H.G., Jr. 1976, Second Reference Catalogue of Bright Galaxies (Austin: Univ. Texas Press) (RC2)
- de Vaucouleurs, G., & Buta, R. 1980, ApJS, 44, 451
- de Vaucouleurs, G., de Vaucouleurs, A., Corwin, H. G., Jr., Buta, R., Paturel, G., & Fouqué, P. 1991, Third Reference Catalogue of Bright Galaxies (Springer, New York) (RC3)
- Edelson, R.A., & Malkan, M.A. 1986, ApJ, 308, 59
- Eggen, O.J., Lynden-Bell, D., & Sandage, A.R. 1962, ApJ, 136, 748
- Elmegreen, D.M., Elmegreen, B.G., & Bellin, A.D. 1990, ApJ, 364, 415
- Elmegreen, D.M., Elmegreen, B.G., Combes, F., & Bellin, A.D. 1992, A&A, 257,17
- Fasano, G., Amico, P., Bertola, F., Vio, R., & Zeilinger, W.W. 1993, MNRAS, 262, 109
- Friedli, D., & Benz, W. 1993, A&A, 268, 65
- Friedli, D., & Benz, W. 1995, A&A, 301, 649
- Granato, G.L., Zitelli, V., Bonoli, F., Danese, L., Bonoli, C., & Delpino, F. 1993, ApJS, 89, 35
- Green, R.F., Schmidt, M., & Liebert, J. 1987, ApJS, 61,305
- Helou, G. 1986, ApJ, 311, L33
- Helou, G., Ryter, C., & Soifer, B.T. 1991, ApJ, 376, 505 (HRS)
- Ho, L.C., Filippenko, A.V., & Sargent, W.L.W. 1997a, ApJS, 112, 315
- Ho, L.C., Filippenko, A.V., & Sargent, W.L.W. 1997b, ApJ, 487, 568
- Ho, L.C., Filippenko, A.V., & Sargent, W.L.W. 1997c, ApJ, 487, 591
- Huchra, J. & Burg, R. 1992, ApJ, 393, 90
- Hunt, L.K. 1991, ApJ, 370, 511
- Hunt, L.K., Malkan, M.A., Moriondo, G., & Salvati, M. 1998, ApJ, January 10, 1999
- Keel, W.C. 1980, AJ, 85, 198
- Keel, W.C. 1993, AJ, 106, 1771
- Kormendy, J., & Richstone, D. 1995, ARA&A, 33, 581
- Kotilainen, J.K., Ward, M.J., Boisson, C., DePoy, D.L., & Smith, M.G., 1992, MNRAS, 256, 149
- Kotilainen, J.K. & Ward, M.J. 1994, MNRAS, 266, 953
- MacKenty, J.W. 1989, ApJ, 343, 125
- MacKenty, J.W. 1990, ApJS, 72, 231
- Maiolino, R., & Rieke, G.H. 1995, ApJ, 454, 95

- Maiolino, R., Ruiz, M., Rieke, G.H., & Papadopoulos, P. 1997, *ApJ*, 485, 552
- Malkan, M.A., Gorjian, V., & Tam, R. 1998, *ApJS*, July, 1998 (MGT)
- Martinet, L. 1995, *Fundamentals of Cosmic Physics*, 15, 341
- Mazzarella, J.M. & Balzano, V. 1986, *ApJS*, 62, 751
- McLeod, K.K. & Rieke, G.H. 1995, *ApJ*, 441, 96
- Miley, G.K., Neugebauer, & Soifer, B.T. 1985, *ApJ*, 293, L11
- Moles, M., Márquez, I., & Pérez 1995, *ApJ*, 438, 604
- Mulchaey, J.S., & Regan, M.W. 1997, *ApJ*, 482, L135
- Norman, C.A., & Scoville, N. 1988, *ApJ*, 332, 124
- Norman, C.A., Sellwood, J.A., & Hasan, H. 1996, *ApJ*, 462, 114
- Odehahn, S., Burstein, D., & Windhorst, R.A. 1997, *AJ*, 114, 2219
- Oliva, E., Origlia, L., Kotilainen, J.K., & Moorwood, A.F.M. 1995, *A&A*, 301, 550
- Pajot, F., Boissé, P., Gispert, R., Lamarre, J.M., Puget, J.L., & Serra, G. 1986, *A&A*, 157, 393
- Persson, C.J. Lonsdale & Helou, G. 1987, *ApJ*, 314, 513
- Pfenniger, D. in *Physics of Nearby Galaxies: Nature or Nurture?*, 1993, T.X. Thuan, C. Balkowski, & J. Tran Thanh Van, eds., Editions Frontieres, Gif-sur-Yvette, 519
- Pfenniger, C., Combes, F., & Martinet, L. 1994, *A&A*, 285, 79
- Piner, B.G., Stone, J.M., & Teuben, P.J. 1995, *ApJ*, 449, 508
- Pompea, S.M., & Rieke, G.H. 1990, *ApJ*, 356, 416
- Roberts, M.S., & Haynes, M.P. 1994, *ARA&A*, 32, 115
- Rowan-Robinson, M., & Crawford, J. 1989, *MNRAS*, 238, 523
- Rush, B., Malkan, M.A., & Spinoglio, L. 1993, *ApJS*, 89, 1 (RMS)
- Rush, B., & Malkan, M.A. 1996, *ApJ*, 456, 466
- Rush, B., Malkan, M.A., Fink, H.H., & Voges, W. 1996, *ApJ*, 471, 190
- Rush, B., Malkan, M.A., & Edelson, R.A. 1996, *ApJ*, 473, 130
- Sandage, A., Freeman, K.C., & Stokes, N.R. 1970, *ApJ*, 160, 831
- Schwarz, M.P. 1981, *ApJ*, 247, 77
- Sellgren, K. 1984, *ApJ*, 277, 623
- Sellwood, J.A., & Wilkinson, A. 1993, *Rep. Prog. Phys.*, 56, 173
- Shlosman, I., Begelman, M.C., & Frank, J. 1990, *Nature*, 345, 679
- Simkin, S.M., Su, H.J., & Schwarz, M.P. 1980, *ApJ*, 237, 404
- Soifer, B.T., Rowan-Robinson, M., Houch, J.R., et al. 1984, *ApJ*, 278, L71
- Soifer, B.T., Sanders, D.B., Madore, B.F., Neugebauer, G., Danielson, G.E., Elias, J.H., Lonsdale, C.J., & Rice, W.L. 1987, *ApJ*, 320, 238
- Soifer, B.T., Boehmer, G., Neugebauer, G., & Sanders, D.B. 1989, *AJ*, 98, 766
- Spinoglio, L., Malkan, M.A., Rush, B., Carrasco, L., & Recillas-Cruz, E. 1995, *ApJ*, 453, 616
- Su, H.J., & Simkin, S.M. . 1980, *ApJ*, 238, L1
- Telesco, C.M. 1988, *ARA&A*, 26, 343
- Terlevich, R., Melnick, J., & Moles, M. 1987, in *Observational Evidence of Activity in Galaxies*, ed. E. Ye. Khachikian, K.J. Fricke, & J. Melnick (Dordrecht:Reidel), 499
- van den Bergh, S. 1998, *Galaxy Morphology and Classification*, (Cambridge University Press: Cambridge)
- Yee, H.K.C. 1983, *ApJ*, 272, 473
- Zitelli, V., Granato, G.L., Mandolesi, N., Wade, R., & Danese, L. 1993, *ApJS*, 84, 185

This 2-column preprint was prepared with the AAS L^AT_EX macros v4.0.

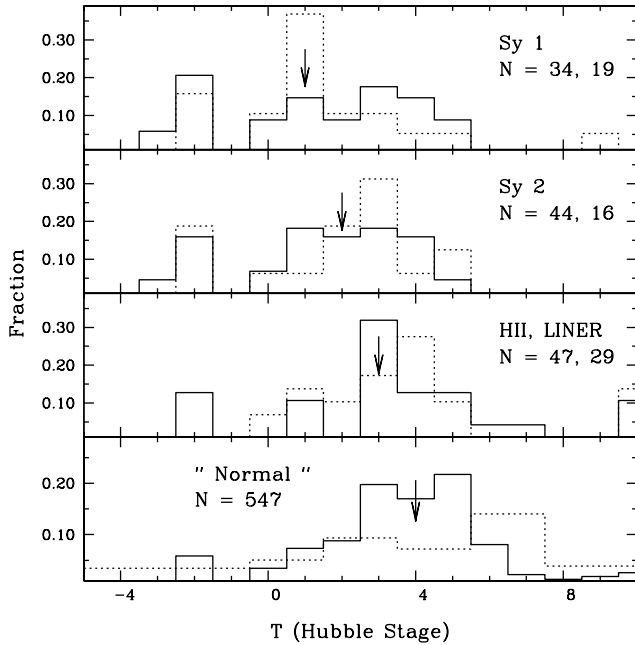


Fig. 1.— Distributions of the morphological type index (Hubble stage). The distributions denoted by a dotted line correspond (from bottom to top) to: 1) the distribution of the Uppsala General Catalog as tabulated by Roberts & Haynes (1994); 2) the $12\mu\text{m}$ LINER sample; 3) the CfA Seyfert 2s; 4) the CfA Seyfert 1s. The numbers given in this and subsequent histograms refer to the number of objects with (in this case) morphological types defined in NED. The two values given in the HII/LINER panel correspond to the HII and LINER subsamples, respectively, and the two values in the Seyfert panels to the $12\mu\text{m}$ and CfA samples. The vertical arrows mark subsample medians, calculated with a type index resolution of unity.

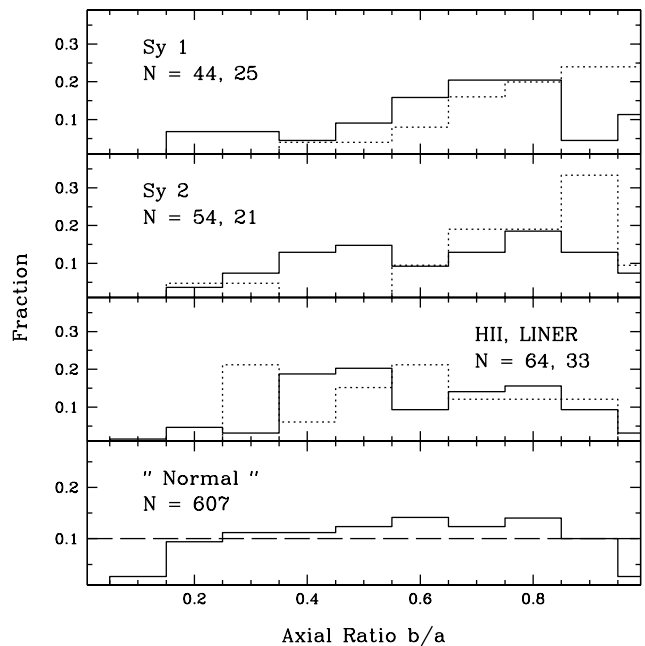


Fig. 2.— Distributions of the axial ratios (b/a). The distributions denoted by a dotted line are the same as those in Fig. 1. Numbers under the panel label give the number of galaxies in each subsample with defined axial ratios. The horizontal dashed line in the lowest panel indicates a random distribution in the absence of optical depth effects, and assuming disks are intrinsically round.

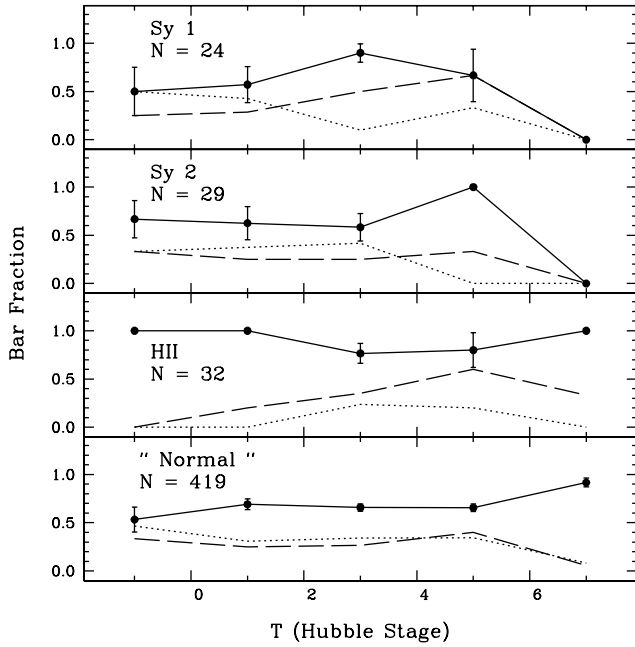


Fig. 3.— Fraction of barred galaxies as a function of Hubble type. The dotted lines shows the unbarred galaxies, the dashed lines the weakly-barred (SAB), and the solid lines the barred (SAB + SB). Error bars are shown only for the barred distributions, and are derived from counting statistics as $\sqrt{f(1-f)/N}$, where f is the fraction of barred objects in a given morphological type bin, and N is the total number of objects in the bin. Numbers under the panel label give the number of galaxies in each subsample with well-defined bar class. The data have been binned as follows: S0a and earlier ($T \leq 0$); Sa, Sab ($0 < T \leq 2$); Sb, Sbc ($2 < T \leq 4$); Sc, Scd ($4 < T \leq 6$); Sd and later ($6 < T$).

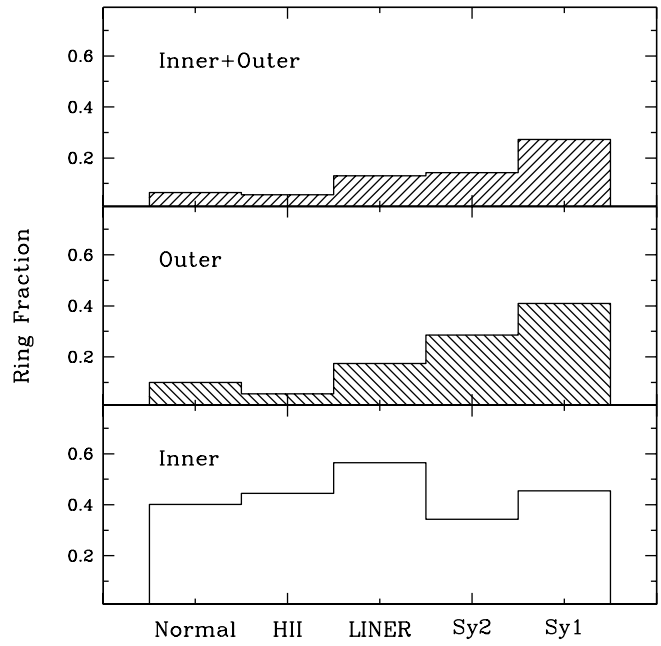


Fig. 4.— Fraction of ringed galaxies as a function of activity class. The lower panel shows inner rings, the middle panel outer ones, and the upper panel those galaxies with both inner and outer rings. Only those objects with ($v < 5000 \text{ km s}^{-1}$) are shown in the figure.

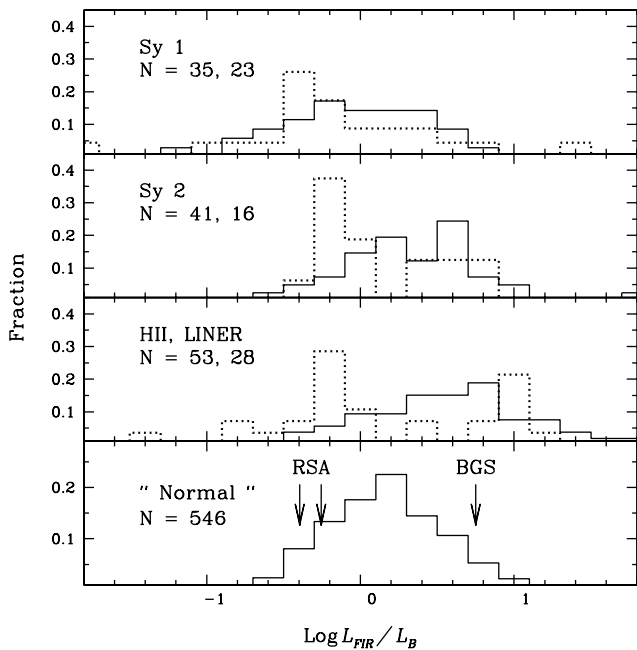


Fig. 5.— Distributions of $\log L_{IR}/L_B$. The distributions denoted by a dotted line are the same as those in Fig. 1. The vertical arrows in the lowest panel mark medians of the unbarred (-0.4) and barred (-0.26) Shapley-Ames galaxies as analyzed by De Jong et al. (1984), and the IRAS Bright Galaxy Sample (Soifer et al. 1987) selected at $60\mu\text{m}$ (0.75).

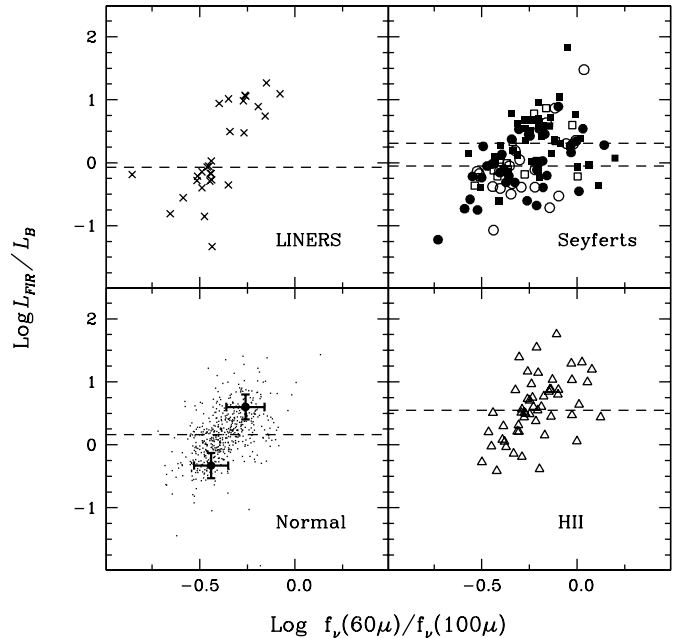


Fig. 6.— Plots of L_{IR}/L_B versus far-infrared flux ratio $f_\nu(60\mu)/f_\nu(100\mu)$; scale is logarithmic. In the upper right panel, the $12\mu\text{m}$ Seyferts are marked with filled symbols (circles for Type 1, squares for Type 2), and the CfA Seyferts with the respective open symbols. In the Normal panel, the two bold data points correspond to the mean and spread in an optically-selected sample (RSA galaxies, de Jong et al. 1984), and in a $60\mu\text{m}$ -selected sample (BGS, Soifer et al. 1989). Each panel contains dashed lines which show the median L_{IR}/L_B for the activity class; in the Seyfert panel, the upper horizontal dashed line marks the median Type 2s, and the lower Type 1s. The two outlying points (upper right) in the Seyfert panel are Arp 220 ($12\mu\text{m}$ Sy2) and Mrk 231 (CfA Sy1).

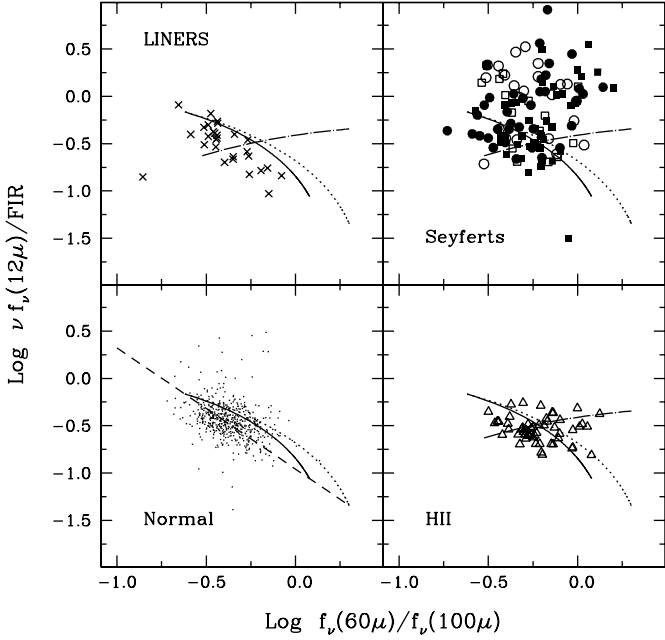


Fig. 7.— Plots of $\Gamma \equiv \nu f_{\nu}(12\mu)/\text{FIR}$ versus $f_{\nu}(60\mu)/f_{\nu}(100\mu)$; scale is logarithmic. In all the panels, the models described in HRS are shown as a solid line and dotted line; the dashed line in the normal panel corresponds to the linear fit for Galactic interstellar medium data given in HRS, and is not reproduced in the other panels. The monotonically-increasing dot-dashed line in the active panels (not shown in the normal panel) represents the trend that would be followed if the colors were dictated by the flux limit at $12\mu\text{m}$ (see HRS). The outlier (lower right) in the Seyfert panel is Arp 220.

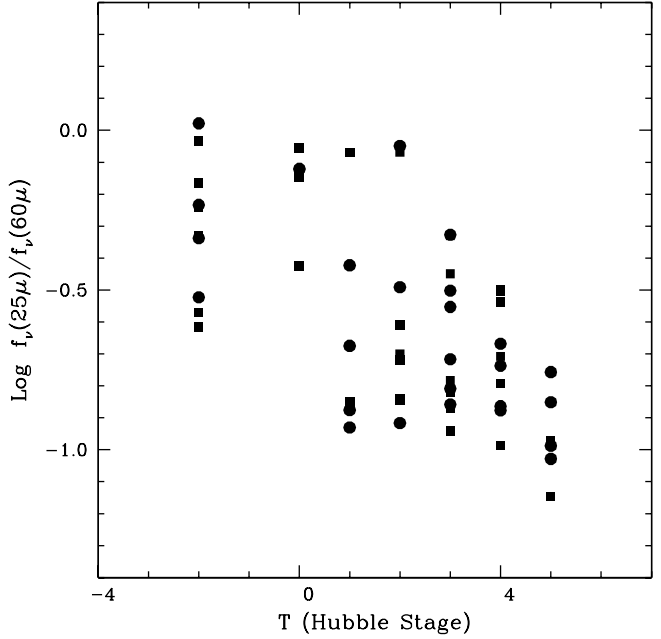


Fig. 8.— Plots of mid-infrared flux ratio $f_{\nu}(25\mu)/f_{\nu}(60\mu)$ versus Hubble type index T for the $12\mu\text{m}$ Seyferts. Seyfert 1s are marked with filled circles, and Type 2s with filled squares. The parametric correlation coefficient for the regression is -0.62 for 28 data points, corresponding to a Student- t statistic of 4.06.